

See discussions, stats, and author profiles for this publication at: <https://www.researchgate.net/publication/231391105>

# Kinetic Investigation of Benzene Ethylation with Ethanol over USY Zeolite in a Riser Simulator

ARTICLE *in* INDUSTRIAL & ENGINEERING CHEMISTRY RESEARCH · DECEMBER 2009

Impact Factor: 2.59 · DOI: 10.1021/ie901526d

---

CITATIONS

11

---

READS

59

## 2 AUTHORS:



Taiwo Odedairo

University of Queensland

34 PUBLICATIONS 159 CITATIONS

SEE PROFILE



Sulaiman al-khattaf

King Fahd University of Petroleum and Min...

117 PUBLICATIONS 1,120 CITATIONS

SEE PROFILE

# Kinetic Investigation of Benzene Ethylation with Ethanol over USY Zeolite in a Riser Simulator

T. Odedairo and S. Al-Khattaf\*

Center of Excellence in Petroleum Refining and Petrochemicals, King Fahd University of Petroleum & Minerals, Dhahran 31261, Saudi Arabia

The ethylation of benzene with ethanol over USY zeolite catalysts has been investigated at three different temperatures (300, 350, and 400 °C) for reaction times of 3, 5, 7, 10, 13, and 15 s with constant benzene to ethanol mole ratio of 1:1. Significant benzene conversion was found in the ethylation of benzene with ethanol over USY-2 catalyst as compared with the negligible conversion observed over USY-1 catalyst of lower acidity. The cracking of ethylbenzene (EB) was found to dominate at high temperatures (350 and 400 °C) in the ethylation of benzene with ethanol over USY-2 catalyst while ethylbenzene ethylation becomes significant at lower temperature (300 °C). Considerable amount of toluene was observed in the ethylation of benzene over USY-2 catalyst and was found to increase with increasing reaction temperature. The effect of reaction conditions on ethylbenzene selectivity, toluene selectivity, toluene-to-EB ratio, and total diethylbenzene (DEB) selectivity, are reported. Kinetic parameters for the ethylation of benzene with ethanol ( $E_1$ ), cracking of EB ( $E_2$ ), ethylation of ethylbenzene with ethanol ( $E_3$ ), and the cracking of diethylbenzene ( $E_4$ ) over USY-2 catalyst were determined using the catalyst activity decay function based on time-on-stream model. The apparent activation energies were found to decrease as follows:  $E_2 > E_3 > E_4 > E_1$ .

## 1. Introduction

Alkylation of benzene is an important reaction in the petrochemical industry.<sup>1,2</sup> Ethylbenzene (EB) is important in the petrochemical industry as an intermediate in the production of styrene, which in turn is used for making polystyrene, a commonly used plastic material.<sup>3</sup> The most important alkylbenzene, ethylbenzene (EB) is predominantly synthesized by alkylation of benzene with ethylene over an acid catalyst.<sup>4,5</sup> The acid catalyst normally used is aluminum chloride, but it is very corrosive and produces a large amount of waste during processing.<sup>6</sup> Solid acid catalysts have recently been developed<sup>7–9</sup> and several acid zeolite catalysts are already used in industry.<sup>10</sup> The vapor phase alkylation of benzene with ethanol in the presence of ZSM-5 zeolites is the famous Mobil-Badger process, which is now in commercial practice for production of ethylbenzene.<sup>11</sup>

The use of zeolite catalysts offers an environmentally friendly route to ethylbenzene and the possibility of achieving superior product selectivity through pore size control.<sup>12,13</sup> Several types of zeolites have been reported to provide high activity in benzene alkylation, for example, faujasite, beta, H-ZSM-5, and MCM-22.<sup>14–20</sup> Faujasites have been employed in alkylation reactions, however, their low resistance to coking limits their industrial use.<sup>21</sup> Y-zeolite is made ultrastable by the removal of aluminum from the framework. The dealumination can be accomplished through the use of steam,<sup>22</sup> acid leaching,<sup>23</sup> or by chemical treatment with hexafluorosilicate or silicon tetrachloride.<sup>24,25</sup> However, the most common procedure is hydrothermal treatment at elevated temperatures under controlled atmosphere (steaming). The resulting ultrastable Y-type zeolites (USY) have modified framework Si/Al ratio, structure, and acidity. They usually exhibit improved reactivity, selectivity, and coking behavior for a catalytic reaction, which is of great interest to petroleum refining industry.<sup>26</sup>

A number of researchers have reported the studies on alkylation reactions over ZSM-type zeolites.<sup>27–32</sup> However, only

a few researchers have performed alkylation reactions over USY-zeolite. Wang et al.<sup>33</sup> studied the alkylation of benzene over three kinds of faujasite-type zeolites from different companies with different SiO<sub>2</sub>/Al<sub>2</sub>O<sub>3</sub> ratios. They found that USH-Y with SiO<sub>2</sub>/Al<sub>2</sub>O<sub>3</sub> ratio of 80 showed the highest conversion, up to 97.8% conversion for 1-dodecene. Yuan et al.<sup>34</sup> investigated the alkylation of benzene over USY zeolite catalyst. The authors found that the catalytic activity and stability depend closely on the pretreatment temperature of catalyst and reaction conditions. The influence of Si/Al ratio of Y-zeolites on the activity and selectivity of benzene alkylation was studied by Nociar et al.<sup>35</sup> They obtained the maximum alkylation activity for Y-zeolite at Si/Al ratio of 7. Alkylation of benzene with long chain alcohols over different Y-type zeolite catalysts has also been reported.<sup>36</sup> Deshmukh et al.<sup>36</sup> reported that the Re–Na–Y catalyst was found to be very effective in the alkylation of benzene with other long chain linear alcohols having 8–18 carbons. Namuangruk et al.<sup>37</sup> investigated the alkylation of benzene over faujasite zeolite using the ONIOM3 model. The model was found to be accurate in predicting adsorption energies of the reactants and product compared to experimental estimates. Barman et al.<sup>38</sup> carried out kinetic studies of benzene alkylation over cerium exchanged NaX zeolite catalyst in which they developed a kinetic model for the reaction based on the Langmuir–Hinshelwood–Hougen–Watson approach with single and dual-site mechanism and reported an activation energy of ~56 kJ/mol. Similarly, Sridevi et al.<sup>11</sup> developed a kinetic model for the reaction based on the Langmuir–Hinshelwood mechanism and found that the activation energy was ~60.03 kJ/mol over AlCl<sub>3</sub>-impregnated 13X zeolites.

From the above discussions, it is clear and evident that less attention has been paid to the kinetic study of benzene ethylation over USY zeolite catalyst. We have not seen any publication with detailed kinetic study on benzene ethylation over USY zeolite catalyst. Therefore, the present study is aimed at investigating the kinetics of ethylation of benzene with ethanol over USY zeolite catalyst in a fluidized-bed reactor by using a

\* To whom correspondence should be addressed. Tel.: +966-3-860-1429. Fax: +966-3- 860-4234. E-mail: skhattaf@kfupm.edu.sa.

quasi-steady-state approximation with catalyst deactivation function based on the time-on-stream (TOS) model, taking into consideration the major side reactions taking place. In addition, the effect of reaction conditions on benzene conversion, ethylbenzene selectivity, diethylbenzene (DEB) selectivity, toluene selectivity, and toluene yield-to-EB yield ratio, will be reported.

## 2. Experimental Section

**2.1. The Riser Simulator.** All the experimental runs were carried out in the riser simulator. This reactor is novel bench scale equipment with internal recycle unit invented by de Lasa.<sup>39</sup> The riser simulator consists of two outer shells, the lower section and the upper section which allow loading or unloading the catalyst easily. The reactor was designed in such a way that an annular space is created between the outer portion of the basket and the inner part of the reactor shell. A metallic gasket seals the two chambers with an impeller located in the upper section. A packing gland assembly and a cooling jacket surrounding the shaft provide support for the impeller. Upon rotation of the shaft, gas is forced outward from the center of the impeller toward the walls. This creates a lower pressure in the center region of the impeller thus inducing flow of gas upward through the catalyst chamber from the bottom of the reactor annular region where the pressure is slightly higher. The impeller provides a fluidized bed of catalyst particles as well as intense gas mixing inside the reactor. A detailed description of various riser simulator components, sequence of injection, and sampling can be found in Kraemer.<sup>40</sup>

The riser simulator consists of two omega CN9000 series temperature controllers that control the vacuum box and reactor temperature. These controllers are calibrated to work with K type omega thermocouples. One of the thermocouples is connected to the catalyst basket, from where the temperature in the reactor is measured. The riser simulator operates in conjunction with series of sampling valves that allow for injection of the feedstock and withdrawal of reaction products in short periods of time. A four-port valve enables the connection and isolation of the 45 cm<sup>3</sup> reactor and the vacuum box, and a six-port valve allows for the collection of a sample of reaction products in a sampling loop. Vacuum box and reactor pressure are displayed on two Omega DP series pressure displays. The pressures are displayed in psia (pounds per square inch absolute). These displays are calibrated for use with Omega pressure transducers, rated for 50 psia maximum pressure. The feedstock was injected into the riser simulator at 14.696 psi (atmospheric pressure). During the state of the feedstock being converted into vapor, an increase in pressure was noticed. After vaporization of the reactant, a further increase in pressure was observed which is due to increased number of molecules, which is as a result of cracking reaction. A drop in pressure was noticed after the stipulated time of reaction.

**2.2. Materials.** Ultrastable Y zeolite (USY) used in this work was obtained from Tosoh Company in the Na form. The zeolite was ion exchanged with NH<sub>4</sub>NO<sub>3</sub> to replace the sodium cation with NH<sub>4</sub><sup>+</sup>. Following this, NH<sub>3</sub> was removed and the H form of the zeolite was spray-dried using kaolin as the filler and silica sol as the binder. Catalysts and Chemicals Industries Co. Japan supplied both materials. The resulting 60- $\mu$ m catalyst particles had the following compositions: 30 wt % zeolite, 50 wt % kaolin, and 20 wt % silica. The process of sodium removal was repeated for the pelletized catalyst. Following this, the catalyst was calcined for 2 h at 600 °C. Finally, the fluidizable catalyst particles (60- $\mu$ m average size) were treated with 100% steam

**Table 1. Characterization of Used Catalysts**

	zeolite	
	USY-1	USY-2
total acidity (mmol/g)	0.033	0.200
unit cell size (Å)	24.28	24.45
SiO <sub>2</sub> /Al <sub>2</sub> O <sub>3</sub>	31.7	10.5
steaming temperature (°C)	800	600
steaming time (h)	6	2
BET surface area (m <sup>2</sup> /g)	155	177
Na <sub>2</sub> O (wt %)	negligible	negligible

at different temperatures and time to obtain the USY zeolites. The steaming conditions of the different USY zeolites are presented in Table 1.

**2.3. Catalyst Characterization.** The BET surface area was measured according to the standard procedure ASTM D-3663 using Sorptomatic 1800 Carlo Erba Strumentazione unit, Italy. The acid property of the catalyst was characterized by NH<sub>3</sub> temperature-programmed desorption (NH<sub>3</sub>-TPD). In all the experiments, 50 mg of sample was outgassed at 400 °C for 30 min in flowing He and then cooled to 150 °C. At that temperature, NH<sub>3</sub> was adsorbed on the sample by injecting pulses of 2  $\mu$ L/pulse. The injection was repeated until the amount of NH<sub>3</sub> detected was the same for the last two injections. After the adsorption of NH<sub>3</sub> was saturated, the sample was flushed at 150 °C for 1 h with He to remove excess NH<sub>3</sub>, and then the temperature was programmed at 30 °C/min up to 1000 °C in flowing helium at 30 mL/min. Flame ionization detector was used to monitor the desorbed NH<sub>3</sub>.

**2.4. Procedure.** Regarding the experimental procedure in the riser simulator, 0.81 g of catalyst was loaded into the riser simulator basket. The system was then sealed and tested for any pressure leaks. Furthermore, the reactor was heated to the desired reaction temperature. The vacuum box was also heated to around 250 °C and evacuated to around 0.5 psi to prevent any condensation of hydrocarbons inside the box. The heating of the Riser Simulator was conducted under continuous flow of argon (inert gas), and it usually takes few hours until thermal equilibrium is finally attained. Before the initial experimental run, the catalyst was activated for 15 min at 620 °C in a stream of air. The temperature controller was set to the desired reaction temperature, in the same manner the timer was adjusted to the desired reaction time. At this point the gas chromatograph was started and set to the desired conditions.

Once the reactor and the gas chromatograph have reached the desired operating conditions, the feedstock was injected directly into the reactor via a loaded syringe. After the reaction, the four port valve immediately opened ensuring that the reaction was terminated and the entire product stream was sent online to the analytical equipment via a preheated vacuum box chamber.

**2.5. Analysis.** The riser simulator operates in conjunction with series of sampling valves that allow, following a pre-determined sequence, one to inject reactants and withdraw products in short periods of time. The products were analyzed in an Agilent model 6890N gas chromatograph with a flame ionization detector and a capillary column INNOWAX, 60-m cross-linked methyl silicone with an internal diameter of 0.32 mm. During the course of the investigation, a number of runs were repeated to check for reproducibility in the experiment results, which were found to be excellent. Typical errors were in the range of  $\pm 2\%$ .

The amount of coke deposited on the spent catalysts was determined by a common combustion method. In this method, a carbon analyzer multi EA 2000 (Analytikjena) is used. Oxygen

is supplied to the unit directly. The multi EA 2000 with CS module is a specially developed system to permit simultaneous or separate determination of the total carbon and total sulfur in samples of solids, pastes, and liquids by means of high temperature oxidation in a current of oxygen. It is based on special HTC (high temperature ceramics) technology which renders a catalyst superfluous. By combining the finely tuned NDIR (nondispersive infrared gas analysis) detection which is selective to CO<sub>2</sub>/SO<sub>2</sub> with the patented VITA (Verweilzeitgekoppelte Integration für TOC-Analysen) procedure, which takes into account the dwelling time, the analysis possible is very precise.

The aliquot of the sample is accurately weighed into the combustion boat and delivered complete into the hot zone of the furnace. There, pyrolysis and oxidation of the sample occurs at a high temperature in the stream of oxygen ( $R + O_2 \rightarrow CO_2 + H_2O$ , where R is a substance with carbon content). The gas produced in the pyrolysis is drawn through a glass tube filled with a specialist desiccant. This desiccation tube also serves as a particle filter, so that no water or dust can get into the detection system of the device. An NDIR detector is used to determine the CO<sub>2</sub> content in the carrier gas. Gases whose molecules are composed of different types of atom possess specific absorption bands in the infrared wavelength range. The concentration of CO<sub>2</sub> is signaled several times per second. An integral over time is created from the series of signals. The integral is proportional to the concentration of carbon in the sample analyzed. A calibration function is then used to calculate the amount of carbon in the sample. The calibration allows for any changes to flow arising over time because of such factors as the aging process, dirt getting into flow regulators, or the desiccants going lumpy, will not automatically necessitate recalibration, which is a positive factor reducing the frequency of desiccant replacement. A small amount of the spent catalyst (0.35 g) is used for the analysis.

### 3. Results and Discussion

**3.1. Catalyst Characterization.** The physicochemical properties of the catalysts used in this study are presented in Table 1. The total acidity for each catalyst was determined by NH<sub>3</sub> adsorption (TPD) and also by the pyridine-adsorption (FTIR) method. Results are summarized in Table 1. It can be seen that USY-2 has 0.200 mmol/g acidity, which is about 6 times higher than that of the USY-1 catalyst.

**3.2. Benzene Ethylation Reaction over USY-1 Catalyst.** The ethylation of benzene with ethanol was carried out at 300, 350, and 400 °C over USY-1 catalyst for residence times of 3, 5, 7, 10, 13, and 15 s with constant benzene to ethanol molar ratio of 1:1. Ethylation of benzene over USY-1 catalyst with SiO<sub>2</sub>/Al<sub>2</sub>O<sub>3</sub> ratio of 31.7 and 0.033 mmol/g of acid sites gave negligible benzene conversion at all temperatures studied. The only product noticed over USY-1 catalyst was ethylbenzene in small amount, with negligible amounts of toluene and diethylbenzene at 400 °C for a reaction time of 15 s. The insignificant benzene conversion observed over USY-1 catalyst is as a result of low concentration of acid sites that is associated with this catalyst.

#### 3.3. Benzene Ethylation Reaction over USY-2 Catalyst.

**3.3.1. Benzene Conversion.** The ethylation of benzene with ethanol over USY-2 catalyst was studied at variable temperature ranges (300, 350, 400 °C) for residence times of 3, 5, 7, 10, 13, and 15 s. The product distributions for benzene ethylation over USY-2 zeolite catalyst under the conditions of the present

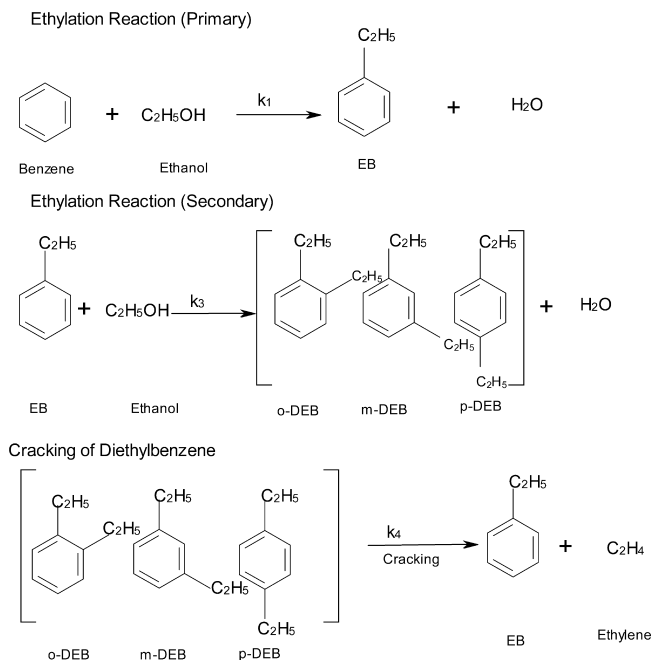
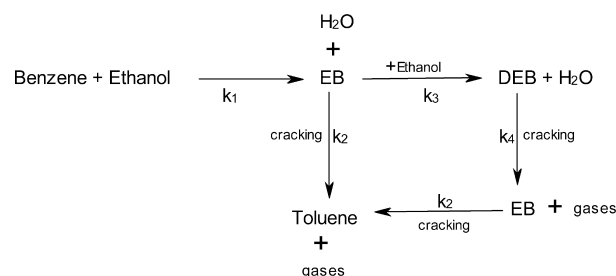


**Figure 1.** Reactions occurring during ethylation of benzene with ethanol over USY-2 catalyst.

**Table 2. Product Distribution (wt %) at Various Reaction Conditions for the Ethylation of Benzene over USY-2 Catalyst**

temp (°C)	time (s)	benzene convn (%)	EB	toluene	m-DEB	p-DEB	o-DEB	total DEB
300	5	2.00	1.44	0.07	0.29	0.15	0.05	0.49
	10	4.85	3.23	0.33	0.78	0.40	0.12	1.31
	15	8.16	5.15	0.67	1.38	0.60	0.22	2.29
350	5	3.03	1.89	0.60	0.29	0.15	0.05	0.49
	10	6.89	4.01	1.62	0.65	0.32	0.11	1.08
	15	11.03	6.15	2.84	0.99	0.49	0.17	1.64
400	5	3.57	1.78	1.29	0.19	0.10	0.03	0.33
	10	8.10	3.76	3.28	0.40	0.21	0.07	0.68
	15	12.13	5.39	5.03	0.55	0.27	0.09	0.92

**Scheme 1**



study were mainly ethylbenzene, toluene and diethylbenzene (Figure 1, Table 2). Traces of *m*-xylene and gaseous hydrocarbons (mainly ethylene) were also observed; however, the yields of these products were consistently very low and as a result were neglected in subsequent analysis. Ethylation reaction was observed to be the major reaction, while at elevated temperatures the cracking reaction is also important. A possible reaction scheme to represent the observed products distribution is shown in Scheme 1. The primary reaction pathway is ethylation of benzene with ethanol to produce EB and water, while the formation of DEB indicates the secondary ethylation step of ethylbenzene with ethanol. Cracking reaction of DEB to produce



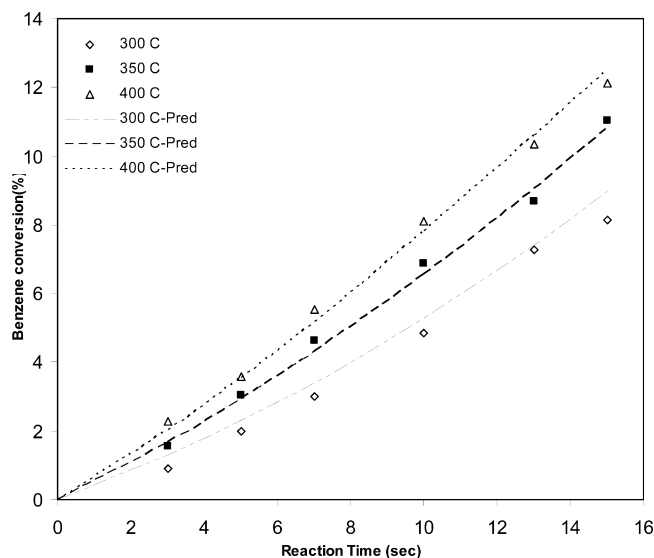


Figure 2. Conversion of benzene with respect to time at various temperatures.

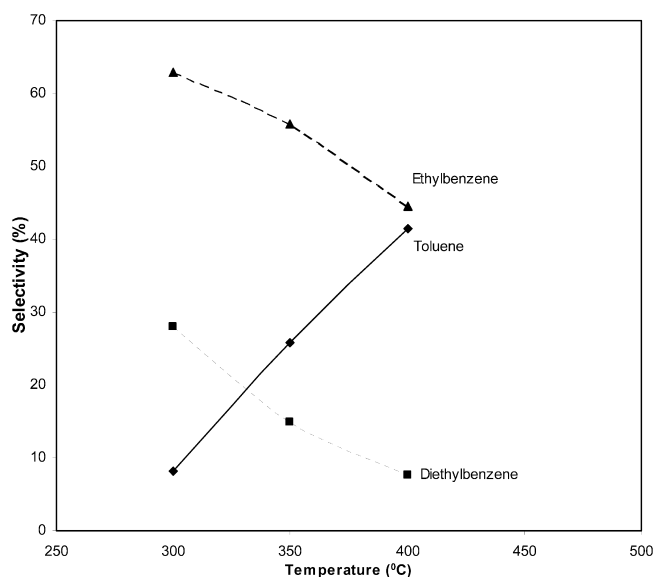


Figure 3. Selectivity of USY-2 catalyst as a function of temperature.

ethylbenzene (EB) and ethylene was also assumed due to the appearance of increased cracking products at elevated temperatures.

The cracking of EB results in the formation of toluene. The cracking reaction involves the formation of 2 mol of toluene and 1 mol of ethylene from 2 mol of ethylbenzene (EB). The product distribution for USY-2 catalyst is given in Table 2. Benzene conversion was found to increase with reaction time and temperature, reaching a maximum of  $\sim 12.1\%$  at 400 °C for a reaction time of 15 s, as shown in Figure 2.

**3.3.2. Ethylbenzene Selectivity.** The effect of temperature on ethylbenzene selectivity for a reaction time of 15 s is shown in Figure 3. As shown in Figure 3, ethylbenzene selectivity decreased steadily with temperature over USY-2 catalyst to a minimum of  $\sim 44.4\%$ . It is evident from the figure that, at 300 °C, less ethylbenzene cracking is occurring, with an ethylbenzene selectivity of  $\sim 62.9\%$ . But as temperature was increased from 300 to 400 °C, more toluene was formed due to ethylbenzene cracking, leading to a decrease in the selectivity of ethylbenzene at higher temperature. This drop suggests that EB undergoes secondary reactions. Moreover, the simultaneous rise in the selectivity of toluene indicates that it is probably the

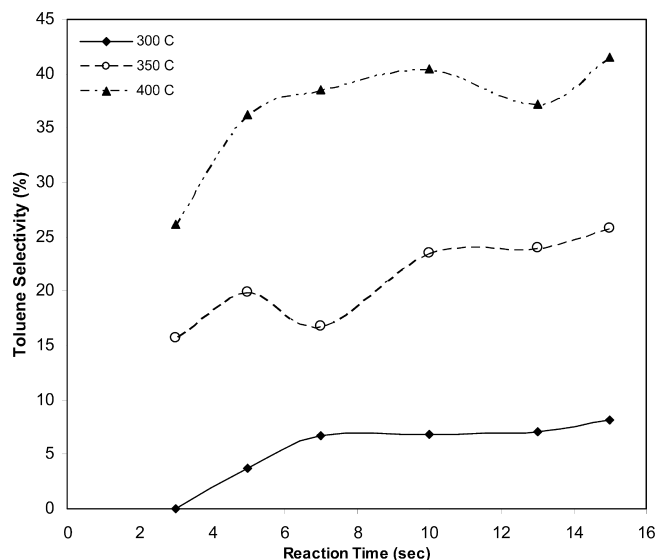


Figure 4. Variation of toluene selectivity with reaction conditions.

products of such secondary reactions. Li et al.<sup>41</sup> observed similar drop in the selectivity of ethylbenzene over HZSM-5-200 and they reported that the decline in EB selectivity can be ascribed to the subsequent side reactions of EB.

**3.3.3. Toluene Selectivity.** Figure 4 shows toluene selectivity with reaction time and temperature over USY-2 catalyst. Toluene selectivity shows a high dependence on temperature over USY-2 catalyst, showing a toluene selectivity rise from 6.85% to 23.58% and then to 40.43% for temperatures of 300, 350, and 400 °C, and for 10 s reaction time, respectively. The selectivity of toluene increased with increase in temperature. The substantial increase in toluene selectivity indicates that the EB formed undergoes cracking at higher temperature, leading to the significant increase in toluene formation at 350 and 400 °C. This is consistent with the observation made by Li et al.<sup>42</sup> that toluene was found to increase significantly as temperature increases, indicating that higher temperature was favorable for the cracking of ethylbenzene to obtain toluene. Similar explanation was given by Gao et al.<sup>43</sup> when traces of toluene were found in the alkylation of benzene with ethanol over ZSM-5-based catalyst. They attributed the formation of toluene to the cracking of ethylbenzene over Brönsted acid sites.

To validate our argument that toluene is been formed from the cracking of EB, we carried out an investigation of EB alone over USY-2 catalyst at the same reaction conditions with that of the ethylation of benzene with ethanol over USY-2 catalyst. It was observed that toluene selectivity of about 18.74% was obtained at 400 °C for a reaction time of 15 s. Similarly, at 350 °C, toluene selectivity of about 10.61% was noticed for a reaction time of 15 s.

The ratio of toluene yield to EB yield has been plotted versus benzene conversion for its ethylation reaction over USY-2 catalyst in Figure 5. The ratio is between 0.05 and 0.12 at 300 °C for the benzene ethylation over USY-2 catalyst. However, as temperature increases, the ratio increased from 0.12 to about 0.93 (i.e., 8 times more). Cracking of the ethylation product (EB) is responsible for the higher toluene-to-EB ratio at higher temperatures.

**3.3.4. Diethylbenzene Selectivity.** Figure 6 shows that the selectivity of diethylbenzene drops from 26.81% to 15.78% and then to 8.43% for the temperatures of 300, 350, and 400 °C for 10 s reaction time, respectively, over USY-2 catalyst. It is evident from Figure 6 that less cracking of diethylbenzene (DEB) to EB is taking place at 300 °C, leading to higher

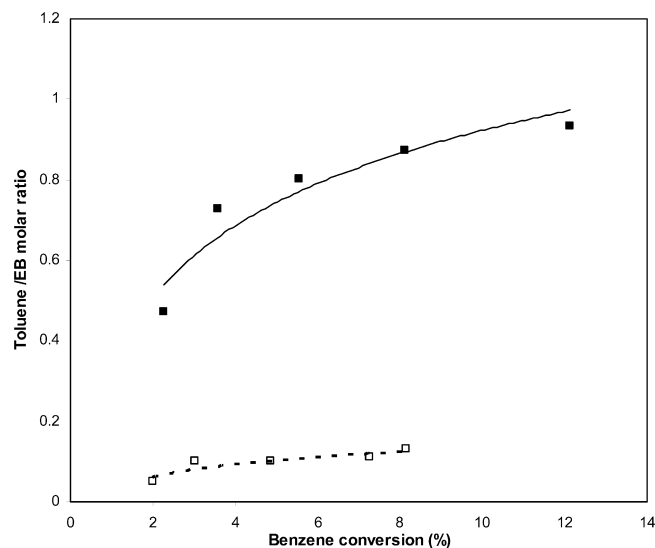


Figure 5. Toluene/EB ratio with benzene conversion at (□) 300 °C and (■) 400 °C.

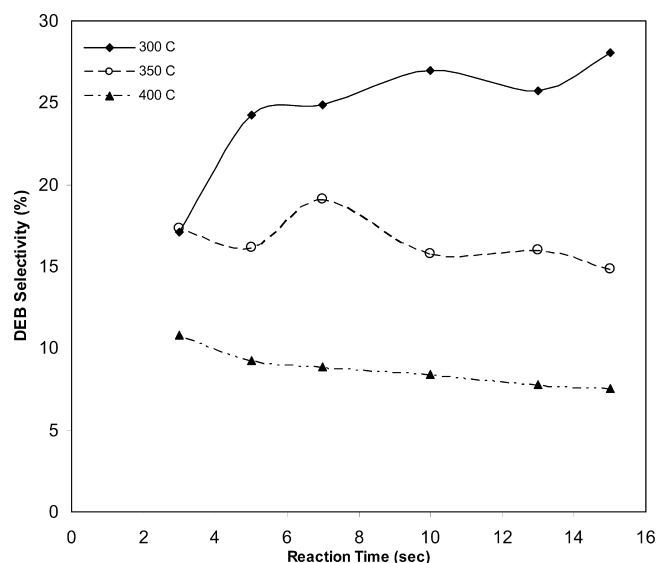


Figure 6. Variation of diethylbenzene selectivity with reaction conditions.

selectivity of diethylbenzene at the lower temperature. The significant decrease in the selectivity of DEB at 350 and 400 °C indicates the cracking of DEB to produce ethylbenzene (EB) and ethylene.

Table 2 shows the distribution of the reaction products for para, meta, and ortho isomers over USY-2 catalyst. Generally, in the case of zeolites this is strongly influenced by the channel geometry and the transport of individual isomers into channel structure.<sup>2</sup> It is clear from the table that, for all the reaction conditions investigated, *meta*-diethylbenzene was found to be higher than the *para*- and *ortho*-diethylbenzene in the ethylation reaction over USY-2 catalyst. However, this is not surprising because it is consistent with the observation made by Raj et al.<sup>2</sup> that medium pore zeolites exhibiting channels with dimensions of about 0.55 nm have led to shape selectivity in the processing of alkyl aromatics, particularly with respect to para isomers of dialkyl aromatic hydrocarbons, while large pore zeolites of the Y, beta, and MCM-22 do not exhibit para selectivity. It can be noticed from Table 2 that, for all the reaction conditions studied; *p/o* ratio was found to be between the range of ~2.73 and ~3.33, while the *p/m* ratio was observed to be between the range of ~0.43 and ~0.53. Kaeding<sup>44</sup> and

Table 3. Coke Formation for Benzene Ethylation with Ethanol at Different Reaction Conditions

temp (°C)	time (s)	convn (%)	coke (USY-2) (wt %)	coke (USY-2)/coke (ZSM-5)
350	5	3.03	0.400	3.150
	10	6.89	0.673	4.487
	15	11.03	0.805	3.546
400 °C	5	3.57	0.402	2.698
	10	8.10	0.690	3.239
	15	12.13	0.887	3.591

Benzene/Ethanol ratio = 1:1.

Halgeri<sup>45</sup> reported that ethylation of ethylbenzene with ethylene/ethanol over ZSM-5 yields a thermodynamic equilibrium mixture of diethylbenzenes (DEBs) (para:meta:ortho = 30:54:16). This gives a *p/o* ratio of 1.875 and *p/m* ratio of 0.56. Therefore, the *p/o* ratios for the EB ethylation reaction under the current experimental conditions are higher than the above equilibrium value, while the *p/m* is almost the same with the equilibrium value stated above.

**3.3.5. Coke Content Measurement.** The coke formation in zeolite has been widely studied<sup>46,47</sup> and depends on the size and shape of the space available near the active sites as well as the diffusion path of the organic molecules in the pores of zeolites. Coke formation can be consecutive or competitive to the reaction leading to the desired product.<sup>48</sup> Coke was also measured at different conditions. Table 3 reveals the amount of coke deposition for different reaction times. From the table, it can be seen that, as reaction time increased from 5 to 15 s, the coke increased from ~0.402 to ~0.887 at 400 °C. Similar increase was noticed at 350 °C. It has been reported that more coke is expected to be deposited on catalysts as the reaction time increases.<sup>48</sup> It is clear that ratio of coke weight percent to percent conversion is small, ranging from 0.073 to 0.132 at all reaction conditions. This implies that the ethylation of benzene with ethanol over USY-2 catalyst is not accompanied by substantial coke deposition.

### 3.4. Benzene Ethylation Reaction over USY-2 Catalyst versus Results of Ethylation Reaction Over ZSM-5-Based Catalyst. 3.4.1. Benzene Conversion.

Ethylation reaction of benzene with ethanol over ZSM-5-based catalyst was reported in our earlier publication.<sup>49</sup> The experimental results showed that the ethylation reaction is the main reaction. Benzene conversions are plotted versus reaction time in Figure 7 at 300, 350, and 400 °C. USY-2 catalyst and ZSM-5-based catalyst showed nearly the same benzene conversion at 300 °C. But as temperature was increased to 350 and 400 °C, a clear difference between the conversions was noticed. Benzene conversion of ~16.95% was obtained at 400 °C for a reaction time of 15 s over ZSM-5-based catalyst with constant benzene to ethanol mole ratio of 1:1 as earlier reported in our recent publication.<sup>49</sup> This conversion is higher than the value obtained over USY-2 catalyst (12.13%) with the same benzene to ethanol mole ratio. The difference in benzene conversion noticed at 350 and 400 °C, is probably due to higher acid strength of ZSM-5 or the smaller crystal size of ZSM-5-based catalyst compared with that of USY-2 catalyst. This is in agreement with the observation made by Du et al.<sup>50</sup> that the conversion of benzene is expected to increase clearly with an increase in catalyst acidity because strong acid sites were required for the activation of carbocations.

**3.4.2. Products Distribution.** Two different reaction mechanisms were observed over USY-2 and ZSM-5-based catalysts, leading to the difference in products selectivity noticed over these catalysts. Ethylation of benzene over ZSM-5-based catalyst was observed to follow a series reaction, in which the ethylation

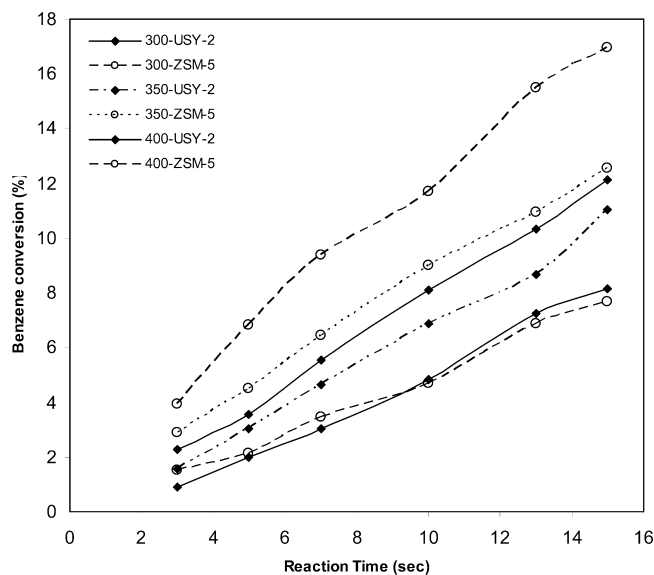


**Figure 7.** Benzene conversion vs reaction time at 300, 350, and 400 °C on catalysts ZSM-5 (○) and USY-2 (◆).

of benzene with ethanol to produce EB represents the primary reaction while the formation of DEB from ethylbenzene ethylation represents the secondary ethylation step. On the other hand, a more complex reaction mechanism was noticed in the ethylation reaction over USY-2 catalyst. The primary reaction pathway is ethylation of benzene with ethanol to produce EB and water. A parallel reaction was then found to occur at both high and low temperatures over this primary product (EB). Ethylbenzene ethylation to produce DEB was found to dominate at low temperature (300 °C), while cracking reaction producing toluene and ethylene becomes significant at higher temperatures. Cracking reaction of DEB to produce ethylbenzene and ethylene was observed at elevated temperatures, while further cracking of EB to produce toluene was also noticed at these temperatures. This is better depicted by the plot of the products selectivity versus reaction temperature for USY-2 catalyst (Figure 3). The selectivity of gaseous hydrocarbons (mainly ethylene) in the ethylation reaction over USY-2 catalyst was found to be ~7.57% at a constant conversion level of 12% at 400 °C compared to ~1.67% obtained in the ethylation reaction over ZSM-5, at the same benzene conversion. Similarly, a selectivity of ~7.37% was noticed at 350 °C over USY-2 compared to ~1.20% observed over ZSM-5, at a constant conversion level of 11%. This observation shows the extent of cracking of ethylation product noticed in the ethylation reaction over USY-2 catalyst compared with ZSM-5.

The product distribution during the ethylation of benzene at 400 °C over ZSM-5 and USY-2 catalyst is compared in Figure 8 at constant conversion level of 12%. The results showed that ethylbenzene has the highest yield over both catalysts. However, considerable amount of toluene was found in the ethylation of benzene with ethanol over USY-2 catalyst as compared to the negligible amount noticed over ZSM-5-based catalyst. Toluene selectivity is about 23 times more over USY-2 catalyst as compared to its selectivity with ZSM-5-based catalyst at 400 °C. All the three isomers of DEB were detected in considerable amount over both catalysts. For all temperatures investigated, *meta*-diethylbenzene was found to be higher than the *para*- and *ortho*-diethylbenzene in the ethylation reaction over USY-2 catalyst. However, for the ethylation reaction over ZSM-5-based catalyst, *para*-diethylbenzene was noticed to be higher than both the *meta*- and *ortho*-diethylbenzene. This observation is expected

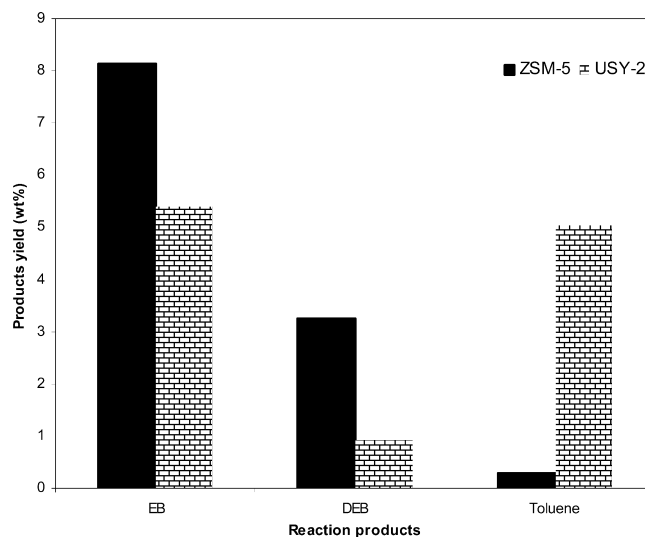


**Figure 8.** Product distribution of benzene ethylation over USY-2 catalyst and ZSM-5 at 12% conversion and 400 °C reaction temperature.

as USY-2 catalyst has been reported not to exhibit para selectivity as explained in section 3.3.3.

**3.4.3. Coke Content Measurement.** The maximum coke formation observed in the ethylation reaction over USY-2 catalyst is ~0.887 as shown in Table 3. This value is approximately 4 times more than the maximum coke deposit noticed in the ethylation of benzene with ethanol over ZSM-5-based catalyst earlier reported.<sup>49</sup> This observation is in agreement with the findings of Corma<sup>10</sup> and other workers<sup>12,51</sup> that, ZSM-5 shows a higher resistance to coking compared with cage-type zeolites like faujasite.

## 4. Kinetic Modeling

**4.1. Model Development for Ethylation Reaction over USY-2.** In this section, a comprehensive kinetic model for benzene ethylation over the USY-2 catalyst was developed. The experimental results were modeled using steady-state approximations with catalyst decay to be a function of TOS. The catalyst activity decay model based on TOS was initially suggested by Voorhies.<sup>52</sup> To develop a suitable kinetic model representing the overall ethylation of benzene, we propose the reaction network shown in Scheme 1. The following set of species balances and catalytic reactions can be written:

Rate of disappearance of benzene,  $r_B$

$$-\frac{V}{W_c} \frac{dC_B}{dt} = k_1 C_B C_E \exp(-\alpha t) \quad (1)$$

Rate of formation of ethylbenzene,  $r_{EB}$

$$\frac{V}{W_c} \frac{dC_{EB}}{dt} = (k_1 C_B C_E - (k_2 C_{EB} + k_3 C_{EB} C_E)) \exp(-\alpha t) \quad (2)$$

Rate of formation of toluene,  $r_T$

$$\frac{V}{W_c} \frac{dC_T}{dt} = k_2 C_{EB} \exp(-\alpha t) \quad (3)$$

Rate of diethylbenzene formation,  $r_{DEB}$

$$\frac{V}{W_c} \frac{dC_{DEB}}{dt} = (k_3 C_{EB} C_E - k_4 C_{DEB}) \exp(-\alpha t) \quad (4)$$

where  $C_B$  is the benzene concentration,  $C_{EB}$  is the concentration of ethylbenzene,  $C_{DEB}$  is the concentration of diethylbenzene,  $C_T$  is the concentration of toluene in the riser simulator,  $V$  is

the volume of the riser (45 cm<sup>3</sup>),  $W_c$  is the mass of the catalyst (0.81 g of catalyst),  $t$  is the time (s),  $\alpha$  is the deactivation constant, and  $k$  is the rate constant (cm<sup>3</sup>/(g of catalyst·s)). By definition the molar concentration,  $C_x$  of every species in the system can be related to its mass fraction,  $y_x$  (measurable from GC), by the following relation:

$$c_x = \frac{y_x W_{hc}}{VMW_x} \quad (5)$$

where  $W_{hc}$  is the weight of feedstock injected into the reactor,  $MW_x$  is the molecular weight of specie  $x$  in the system,  $V$  is the volume of riser simulator.

It should be noted that the following assumptions were made in deriving the reaction network: (1) The cracking of ethylbenzene follows simple first-order kinetics, while the ethylation reactions follow second order kinetics. (2) An irreversible reaction path is assumed for both the ethylation and cracking reactions. Sridevi et al.<sup>11</sup> made similar assumption since the conversion of benzene is small. (3) Catalysts deactivation is assumed to be a function of TOS. A single deactivation function is defined for all the reactions taking place. (4) Isothermal operating conditions can also be assumed given the design of the riser simulator unit and the relatively small amount of reacting species.<sup>39</sup> This is justified by the negligible temperature change observed during the reactions. (5) A pseudo-first-order reaction kinetic for all species involved in the reactions. (6) Negligible thermal conversion.

Substituting eq 5 into eqs 1–4 gives the following first order differential equations which are in terms of weight fractions of the species:

$$\frac{dy_B}{dt} = -A_1 k_1 y_B y_E \frac{W_c}{V} \exp(-\alpha t) \quad (6)$$

$$\frac{dy_{EB}}{dt} = [A_2 k_1 y_B y_E - (k_2 y_{EB} + A_1 k_3 y_{EB} y_E)] \frac{W_c}{V} \exp(-\alpha t) \quad (7)$$

$$\frac{dy_T}{dt} = A_3 k_2 y_{EB} \frac{W_c}{V} \exp(-\alpha t) \quad (8)$$

$$\frac{dy_{DEB}}{dt} = (A_4 k_3 y_{EB} y_E - k_4 y_{DEB}) \frac{W_c}{V} \exp(-\alpha t) \quad (9)$$

$A_1$ ,  $A_2$ ,  $A_3$ , and  $A_4$  are lumped constants given below.

$$\begin{aligned} A_1 &= \frac{W_{hc}}{VMW_E} \\ A_2 &= \frac{MW_{EB} W_{hc}}{VMW_B MW_E} \\ A_3 &= \frac{MW_T}{MW_{EB}} \\ A_4 &= \frac{MW_{DEB} W_{hc}}{VMW_{EB} MW_E} \end{aligned}$$

Equations 6–9 contain nine parameters,  $k_1$ – $k_4$ ,  $E_1$ – $E_4$ , and  $\alpha$ , which are to be determined by fitting into experimental data.

The temperature dependence of the rate constants was represented with the centered temperature form of the Arrhenius equation, that is,

$$k_i = k_{oi} \exp \left[ \frac{-E_i}{R} \left( \frac{1}{T} - \frac{1}{T_o} \right) \right] \quad (10)$$

Since the experimental runs were done at 300, 350, and 400 °C,  $T_o$  was calculated to be 350 °C. Where  $T_o$  is an average temperature introduced to reduce parameter interaction,<sup>53</sup>  $k_{oi}$  is the rate constant for reaction  $i$  at  $T_o$ ,  $W_c$  is the weight of catalyst, and  $E_i$  is the activation energy for reaction  $i$ .

**4.2. Discussion of Kinetic Modeling Results.** The kinetic parameters  $k_{oi}$ ,  $E_i$ , and  $\alpha$  for the ethylation reaction were obtained using nonlinear regression (MATLAB package). Table 4 reports the parameters obtained along with the corresponding 95% confidence limits, while Tables 5–8 presents the correlation matrices for the parameters. The correlation matrices of the regression analysis show that the parameters are highly correlated. From the results of the kinetic parameters presented in Table 4, it is observed that catalyst deactivation was found to be small,  $\alpha = 0.0776$ , indicating low coke formation in agreement with the data shown in Table 3 indicating very low coke yield. This value is higher than  $\alpha$  (0.0250) reported by Odedairo and Al-Khattaf<sup>49</sup> over ZSM-5-based catalyst for benzene to ethanol mole ratio of 1:1. This significant result is in perfect agreement with the findings of refs 10, 12 and 51 in which the authors reported that cage-type zeolites like faujasite shows a lower resistance to coking compared with ZSM-5-based catalyst. It was also observed that the ratio of the coke weight percent in the ethylation reaction over USY-2 catalyst to coke weight percent in the ethylation reaction over ZSM-5 earlier reported was noticed to be between the range of 2.7 and 4.5 as shown in Table 3. It was observed that the ratio of catalyst deactivation constant for both catalysts ( $\alpha_{(USY-2)}/\alpha_{(ZSM-5)}$ ) is 3.10, which is in the same range of the coke ratio of the two catalysts. This observation confirms that the catalyst deactivation in both catalysts is directly related to coke deposition.

Apparent activation energies of 27.21, 24.71, 16.32, and 15.39 kJ/mol were obtained for the cracking of EB, ethylbenzene ethylation, cracking of DEB, and benzene ethylation, respectively. It can be seen from the table that the apparent activation energies for the benzene ethylation, cracking of DEB, ethylbenzene ethylation, and cracking of EB follows the increasing order:  $E_1 < E_4 < E_3 < E_2$ . Odedairo and Al-Khattaf<sup>49</sup> recently reported apparent energies of activation of 34.69 kJ/mol for benzene ethylation over ZSM-5-based catalyst and 9.53 kJ/mol for the secondary ethylation reaction.

The apparent activation energy obtained for benzene ethylation over ZSM-5-based catalyst (34.69 kJ/mol) earlier reported is higher than the 15.39 kJ/mol obtained in the present study over USY-2 catalyst. Looking to their pore opening and their pore geometry, this result is not surprising. USY-2 catalyst with a diameter of 7.4 Å and the free diameter inside the cages of 12 Å is large enough for the reactants and reaction products as compared to the medium pore zeolite (ZSM-5) with almost the same critical diameter with benzene. Therefore, the activation energy for benzene diffusion ( $E_D$ ) over ZSM-5-based catalyst is greater than the  $E_D$  in USY-2 catalyst. According to Levenspiel<sup>54</sup> the apparent activation energy ( $E_{App}$ ) is equivalent to half of the summation of the intrinsic activation energy ( $E_{in}$ ) and the diffusion activation energy ( $E_D$ ) as follows:

$$E_{App} = \frac{E_{in} + E_D}{2}$$

Since  $E_{D(ZSM-5)} > E_{D(USY-2)}$ , therefore the apparent activation energy for benzene ethylation over ZSM-5 ( $E_{App-ZSM-5}$ ) is greater



**Table 4. Estimated Kinetic Parameters Based on Time-on-Stream (TOS Model)**

	values				
parameters	$k_1$	$k_2$	$k_3$	$k_4$	$\alpha$
$E_i$ (kJ/mol)	15.39	27.21	24.71	16.32	0.0776
95% CL	1.51	6.92	7.39	12.85	0.0088
$k_0^a \times 10^3$	0.0102	1.0775	0.1266	10.6285	
[m <sup>3</sup> /(kg of catalyst·s)]					
95% CL $\times 10^3$	0.0006	0.1208	0.0177	2.5213	

<sup>a</sup> Pre-exponential factor as obtained from eq 10; unit for second order (m<sup>6</sup>/kg of catalyst·s).

**Table 5. Correlation Matrix for Benzene Ethylation (TOS Model) (Feed Ratio = 1:1 (Benzene:Ethanol))**

	$k_1$	$E_1$	$\alpha$
$k_1$	1.0000	-0.1016	0.9542
$E_1$	-0.1016	1.0000	-0.0607
$\alpha$	0.9542	-0.0607	1.0000

**Table 6. Correlation Matrix for Ethylbenzene Cracking (TOS Model)**

	$k_2$	$E_2$	$\alpha$
$k_2$	1.0000	-0.3245	0.7577
$E_2$	-0.3245	1.0000	-0.0886
$\alpha$	0.7577	-0.0886	1.0000

**Table 7. Correlation Matrix for Ethylbenzene Ethylation (TOS Model)**

	$k_3$	$E_3$	$\alpha$
$k_3$	1.0000	-0.4895	0.7298
$E_3$	-0.4895	1.0000	-0.1122
$\alpha$	0.7298	-0.1122	1.0000

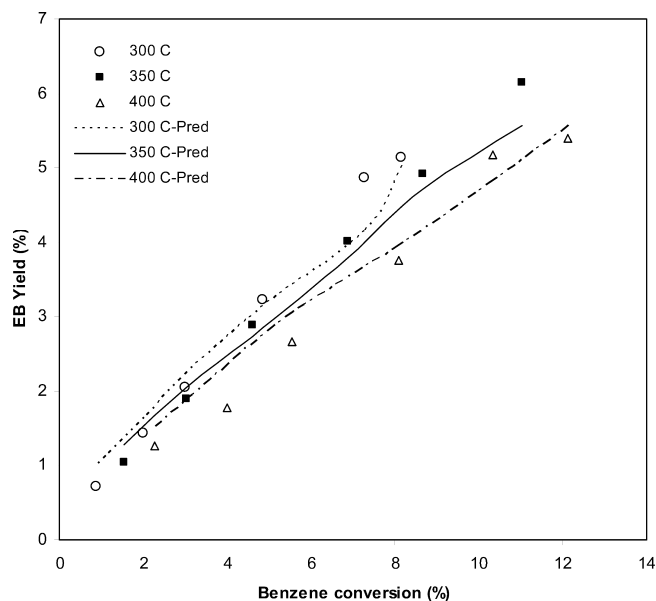
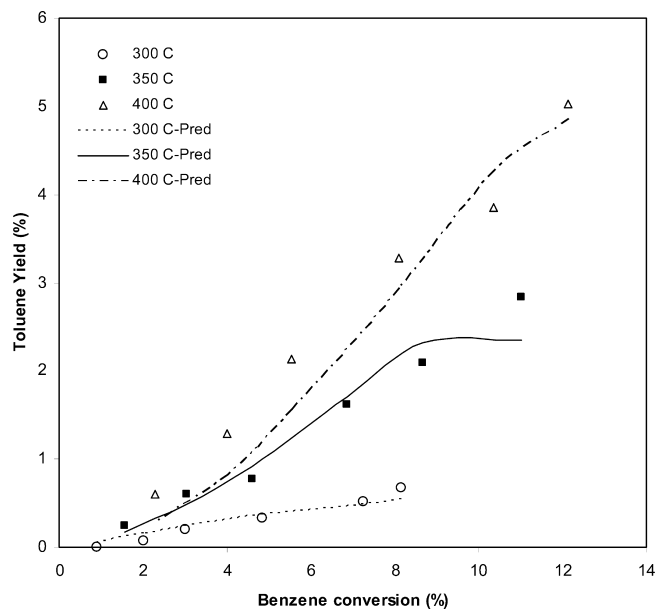
**Table 8. Correlation Matrix for Diethylbenzene Cracking (TOS Model)**

	$k_4$	$E_4$	$\alpha$
$k_4$	1.0000	-0.1880	0.6935
$E_4$	-0.1880	1.0000	-0.0627
$\alpha$	0.6935	-0.0627	1.0000

than the apparent activation energy for benzene ethylation over USY-2 catalyst ( $E_{\text{App-USY-2}}$ ).

It is of great interest to note that the apparent activation energy for ethylbenzene cracking (27.21 kJ/mol) is higher than the apparent energy of activation for benzene ethylation (15.39 kJ/mol). This clearly suggests that an increase in temperature leads to a larger fraction of cracking products, as shown in Table 2. Similar explanation was given by Atias et al.<sup>55</sup> during the catalytic conversion of 1,2,4-trimethylbenzene when a higher apparent energy of activation was obtained for the isomerization of 1,2,4-TMB as compared with its disproportionation. The lower apparent energy of activation obtained for benzene ethylation indicates that the ethylation reaction is less sensitive to temperature variations. Therefore, EB formation is not expected to change significantly with temperature, as shown in Table 2.

The apparent activation energy ( $E_2$ ) of 27.21 kJ/mol was obtained for the formation of toluene during the cracking of EB over USY-2 catalyst. This value is higher than the 16.32 kJ/mol obtained for the cracking of DEB ( $E_4$ ). This indicates that the activation energy required to form toluene as a result of ethylbenzene cracking is higher than the apparent activation energy required for removing an ethyl group from diethylbenzene as a result of DEB cracking by magnitudes of 10–11 kJ/mol. From a comparison of the apparent activation energies for ethylbenzene ethylation (9.53 kJ/mol) over ZSM-5-based catalyst earlier reported and ethylbenzene ethylation (24.71 kJ/mol)

**Figure 9.** Ethylbenzene yield vs benzene conversion at various temperatures.**Figure 10.** Toluene yield vs benzene conversion at various temperatures.

over USY-2 catalyst, the difference in the apparent activation energies over the two catalysts is probably due to the formation of DEB within the pores of USY-2 catalyst as compared with the formation of DEB on the crystal surface of ZSM-5-based catalyst.

To check the validity of the estimated kinetic parameters for use under conditions beyond those of the present study, the fitted parameters were substituted into the comprehensive model developed for this scheme and the equations were solved numerically using the fourth-order-Runge–Kutta routine. The numerical results were compared with the experimental data as shown in Figure 2. It can be observed from this figure that the calculated results compare very well with the experimental data. Further comparisons between model predictions and experimental data are presented in Figures 9 and 10. It can be seen that the model predictions compared very well with the experimental data. This demonstrates that the proposed kinetic model fits well into our experimental observations. In addition, the reconciliation plot (Figure 11) between the experimental data

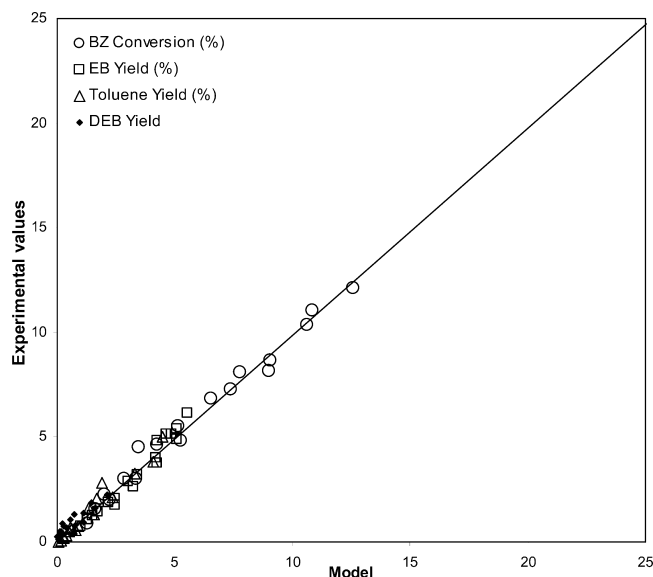


**Figure 11.** Overall comparison between the experimental results and model predictions.

and the model predictions display a normal distribution of residuals, besides, the adequacy of the model and the selected parameters to fit the data as shown in Table 4 gave 0.9830 regression coefficients.

## 5. Conclusions

The following conclusions can be drawn from the ethylation reaction of benzene with ethanol over the USY zeolite catalysts. The study was carried out over the temperature range of 300–400 °C.

(1) Y-zeolite acidity plays a major role in benzene conversion. Significant benzene conversion was achieved over USY-2 catalyst as compared to the negligible benzene conversion observed over USY-1 catalyst even at high temperatures.

(2) Toluene was found in considerable amount in the ethylation of benzene with ethanol over USY-2 catalyst. It is worth mentioning that toluene was not observed over USY-1 catalyst at all conversion levels.

(3) A parallel reaction was noticed over the primary ethylation product (EB) using USY-2 catalyst. Ethylbenzene ethylation was found to dominate at low temperature (300 °C), while cracking reaction becomes significant at higher temperatures (350 and 400 °C).

(4) Kinetic parameters for the benzene–ethanol system during their ethylation reaction ( $E_1$ ), cracking of EB ( $E_2$ ), ethylation of ethylbenzene with ethanol ( $E_3$ ), and the cracking of DEB ( $E_4$ ) over USY-2 catalyst have been calculated using the catalyst activity decay function based on TOS. The apparent activation energies were found to decrease as follows:  $E_2 > E_3 > E_4 > E_1$ .

(5) Comparison between ethylation reaction over USY-2 catalyst and the ethylation reaction over ZSM-5 earlier reported showed that, toluene selectivity is about 23 times more over USY-2 catalyst as compared to its selectivity with ZSM-5 at 400 °C.

(6) Coke formation observed in the ethylation reaction over USY-2 catalyst was found to be ~4 times more than the coke deposit noticed over ZSM-5-based catalyst earlier reported.

## Acknowledgment

The authors would like to express their appreciation to King AbdulAziz City for Science and Technology (KACST) for their

financial support. Also, the support of the King Fahd University of Petroleum and Minerals is highly appreciated. Mr. Mariano Gica also is acknowledged for his help during the experimental work.

## Nomenclature

$C_i$  = concentration of specie  $i$  in the riser simulator (mol/m<sup>3</sup>)

CL = confidence limit

$E_i$  = apparent activation energy of  $i$ th reaction (kJ/mol)

$E_D$  = activation energy for benzene diffusion (kJ/mol)

$E_{in}$  = activation energy for benzene ethylation (kJ/mol)

$k_i$  = apparent rate constant for the  $i$ th reaction (m<sup>3</sup>/kg<sub>cat</sub>·s)

$k_1$  = rate constant of reaction 1 (m<sup>3</sup>/kg<sub>cat</sub>·s)

$k_2$  = rate constant of reaction 2 (m<sup>3</sup>/kg<sub>cat</sub>·s)

$k_3$  = rate constant of reaction 3 (m<sup>3</sup>/kg<sub>cat</sub>·s)

$k_4$  = rate constant of reaction 4 (m<sup>3</sup>/kg<sub>cat</sub>·s)

$k_0$  = Pre-exponential factor in Arrhenius equation defined at an average temperature [m<sup>3</sup>/kg<sub>cat</sub>·s), units based on first order reaction

$MW_i$  = molecular weight of specie  $i$

$R$  = universal gas constant (kJ/(kmol K))

$t$  = reaction time (s)

$T$  = reaction temperature (K)

$T_0$  = average temperature of the experiment (350 °C)

$V$  = volume of the riser (45 cm<sup>3</sup>)

$W_c$  = mass of the catalysts (0.81 g cat)

$W_{hc}$  = total mass of hydrocarbons injected in the riser (0.162 g)

$y_i$  = mass fraction of  $i$ th component (wt %)

## Subscripts

0 = at time  $t = 0$

1 = for reaction (1)

2 = for reaction (2)

3 = for reaction (3)

4 = for reaction (4)

cat = catalyst

$i$  = for  $i$ th component

## Chemical species

W = water

E = ethanol

B = benzene

EB = ethylbenzene

DEB = diethylbenzene

T = toluene

## Greek Letter

$\alpha$  = apparent deactivation constant (s<sup>-1</sup>) (TOS model)

## Literature Cited

- (1) Vijayaraghavan, V. R.; Raj, K. J. A. Ethylation of benzene with ethanol over substituted large pore aluminophosphate-based molecular sieves. *J. Mol. Catal. A* **2004**, *207*, 41.
- (2) Raj, K. J. A.; Padma Malar, E. J.; Vijayaraghavan, V. R. Shape-selective reactions with AEL and AFI-type molecular sieves alkylation of benzene, toluene, and ethylbenzene with ethanol, 2-propanol, methanol and *t*-butanol. *J. Mol. Catal. A* **2006**, *243*, 99–105.
- (3) Cejka, J.; Wichterlova, B. Acid-catalyzed synthesis of mono- and dialkylbenzenes over zeolites: Active sites, zeolite topology, and reaction mechanisms. *Catal. Rev.* **2002**, *44*, 375.
- (4) Cheng, J. C.; Degnan, T. F.; Beck, J. S.; Huang, Y. Y.; Kalyanaraman, M.; Kowalski, J. A.; Loehr, C. A.; Mazzone, D. N. A comparison of zeolites MCM-22, beta, and USY for liquid phase alkylation of benzene with ethylene. *Stud. Surf. Sci. Catal.* **1999**, *121*, 53–60.
- (5) Lenarda, M.; Storaro, L.; Pellegrini, G.; Piovesan, L.; Ganzeria, R. Solid acid catalysts from clays. Part 3: benzene alkylation with ethylene catalyzed by aluminium and aluminium gallium pillared bentonites. *J. Mol. Catal. A* **1999**, *145*, 237–244.

- (6) Benthams, M. F.; Gajda, G. J.; Jensen, R. H.; Zinnen, H. A. *Erdgas Kohle*. **1997**, 113, 84.
- (7) Selvaraj, M.; Pandurangan, A.; Seshadri, K. S.; Sinha, P. K.; Lal, K. B. Synthesis, characterization and catalytic application of MCM-41 mesoporous molecular sieves containing Zn and Al. *Appl. Catal., A* **2003**, 242, 347–364.
- (8) Perego, C.; Amarilli, S.; Carati, A.; Flego, C.; Pazzuconi, G.; Rizzo, C.; Bellussi, G. Mesoporous silica-aluminas as catalyst for the alkylation of aromatic hydrocarbons with olefins. *Microporous Mesoporous Mater.* **1999**, 27, 345–354.
- (9) J. Cejka, J.; Kapustin, G. A.; Wichterlova, B. Factors controlling iso-selectivity/*N*-selectivity and para-selectivity in the alkylation of toluene with isopropanol on molecular-sieves. *Appl. Catal., A* **1994**, 108, 187–204.
- (10) Corma, A. Inorganic solid acids and their use in acid-catalyzed hydrocarbon reactions. *Chem. Rev.* **1995**, 95, 559.
- (11) Sridevi, U.; Bhaskar Rao, B. K.; Narayan C., Pradhan. Kinetics of alkylation of benzene with ethanol on  $\text{AlCl}_3$ -impregnated 13X zeolites. *Chem. Eng. J.* **2001**, 83, 185–189.
- (12) Chen, N. Y.; Garwood, W. E. Industrial application of shape-selective catalysis. *Catal. Rev. Sci. Eng.* **1986**, 28, 185–264.
- (13) Corma, A.; Domine, M. E.; Valencia, S. Water-resistant solid Lewis acid catalysts: Meerwein-Ponndorf-Verley and Oppenauer reactions catalyzed by tin-beta zeolite. *J. Catal.* **2003**, 215, 294–304.
- (14) Degnan, T. F.; Smith, C. M.; Venkat, C. R. Alkylation of aromatics with ethylene and propylene: Recent developments in commercial processes. *Appl. Catal., A* **2001**, 221, 283–294.
- (15) Venuto, P. B.; Hamilton, L. A.; Landis, P. S.; Wise, J. J. Organic reactions catalyzed by crystalline aluminosilicates. 1. Alkylation reaction. *J. Catal.* **1966**, 5, 484.
- (16) Corma, A.; Martinez-Soria, V.; Schnoefeld, E. Alkylation of benzene with short-chain olefins over MCM-22 zeolite: Catalytic behavior and kinetic mechanism. *J. Catal.* **2000**, 192, 163–173.
- (17) Becker, K. A.; Karge, H. G.; Streubel, W. D. Benzene alkylation with ethylene and propylene over H-mordenite as catalyst. *J. Catal.* **1973**, 28, 403–413.
- (18) Smirniotis, P. G.; Ruckenstein, E. Alkylation of benzene or toluene with MeOH or  $\text{C}_2\text{H}_4$  over ZSM-5 or  $\beta$  zeolite: Effect of the zeolite pore openings and of the hydrocarbons involved on the mechanism of alkylation. *Ind. Eng. Chem. Res.* **1995**, 34, 1517.
- (19) Reddy, K. S. N.; Rao, B. S.; Shiralkar, U. P. Alkylation of benzene with isopropanol over zeolite beta. *Appl. Catal., A* **1993**, 95, 53–63.
- (20) Weitkamp, J. International Symposium in Zeolite Catalysis, Siófok, Hungary. *Acta Phys. Chem.* **1985**, 217.
- (21) Smirniotis, P. G.; Ruckenstein, E. Alkylation of benzene of toluene with MeOH or  $\text{C}_2\text{H}_4$  over ZSM-5 or  $\beta$  zeolite. *Ind. Eng. Chem. Res.* **1995**, 34, 1517–1528.
- (22) Stach, H.; Lohse, U.; Thamm, H.; Schirmer, W. Adsorption equilibria of hydrocarbons on highly dealuminated zeolites. *Zeolite 6* **1986**, 74–90.
- (23) Gola, A.; Rebours, B.; Milazzo, E.; Lynch, J.; Benazzi, E.; Lacombe, S.; Delevoye, L.; Fernandez, C. Effect of leaching agent in the dealumination of stabilized Y-zeolites. *Microporous Mesoporous Mater.* **2000**, 40, 73–83.
- (24) Lonyi, F.; Lunsford, J. H. The development of strong acidity in hexafluorosilicate-modified Y-type zeolite. *J. Catal.* **1992**, 136, 566–577.
- (25) Kubelkova, L.; Seidl, V.; Novakova, J.; Bednarova, S.; Jiru, P. Properties of Y-type zeolite with various silicon aluminium ratio obtained by dealumination with silicon tetrachloride—Distribution of aluminium and hydroxyl-groups and interaction with ethanol. *J. Chem. Soc., Faraday Trans.* **1984**, 80, 1367.
- (26) Al-Khattaf, S.; Iliyas, A.; Al-Amer, A.; Inui, T. The effect of Y-zeolite acidity on m-xylene transformation reactions. *J. Mol. Catal. A* **2005**, 225, 117–124.
- (27) Anderson, J. R.; Fogar, K.; Mole, T.; Rajyadhyaksha, R. A.; Sanders, J. V. Reactions on ZSM-5-type zeolite catalysts. *J. Catal.* **1979**, 58, 114–130.
- (28) Anderson, J. R.; Mole, T.; Christov, V. Mechanism of some conversions over ZSM-5 catalysts. *J. Catal.* **1980**, 61, 477–484.
- (29) Bhat, Y. S.; Halgeri, A. B.; Prasada Rao, T. S. R. Kinetics of toluene alkylation with methanol on HZSM-8 zeolite catalysts. *Ind. Eng. Chem. Res.* **1998**, 28, 894–899.
- (30) Chandavar, K. H.; Kulkarni, S. B.; Ratnaswamy, P. Alkylation of benzene with ethyl alcohol over ZSM-5 zeolites. *Appl. Catal.* **1982**, 4, 287–295.
- (31) Lee, B.; Wang, I. Kinetic analysis of ethylation of toluene on HZSM-5. *Ind. Eng. Chem. Prod. Res. Dev.* **1985**, 24, 201–208.
- (32) Fraenkel, D.; Levy, M. Comparative study of shape-selective toluene alkylation over HZSM-5. *J. Catal.* **1989**, 118, 10–21.
- (33) Wang, B.; Lee, C. W.; Cai, T.; Park, S. Benzene alkylation with 1-dodecene over Y-zeolite. *Bull. Korean Chem. Soc.* **2001**, 22, 9.
- (34) Yuan, X. D.; Park, J. N.; Wang, J.; Lee, C. W.; Park, S. E. Alkylation of benzene with 1-dodecene over USY zeolite catalyst: Effect of pretreatment and reaction conditions. *Korean J. Chem. Eng.* **2002**, 19, 607–610.
- (35) Nociar, A.; Hudec, P.; Jakubik, T.; Smieskova, A.; Zidek, Z. Alkylation of benzene by linear  $\alpha$ -olefins  $\text{C}_{16}$  over dealuminated Y-zeolites and mordenites. *Pet. Coal* **2003**, 45, 3–4.
- (36) Deshmukh, A. R. A. S.; Gumaste, V. K.; Bhawal, B. M. Alkylation of benzene with long chain (C8–C18) linear primary alcohols over Y-zeolite. *Catal. Lett.* **2000**, 64, 247–250.
- (37) Namuangruk, S.; Pantu, P.; Limtrakul, J. Alkylation of benzene with ethylene over faujasite zeolite investigated by the ONIOM method. *J. Catal.* **2004**, 225, 523–530.
- (38) Barman, S.; Pradhan, N. C.; Basu, J. K. Kinetics of alkylation of benzene with ethyl alcohol catalyzed by Ce-exchanged NaX zeolite. *Ind. Chem. Eng., Sect. A* **2006**, 48, 1.
- (39) de Lasa, H. I. Riser simulator for catalytic cracking studies. U.S. Patent 5, 1991, 102,628.
- (40) Kraemer, D. W. Ph.D. Dissertation. University of Western Ontario, London, Canada, 1991.
- (41) Li, Y.; Xue, B.; Yang, Y. Synthesis of ethylbenzene by alkylation of benzene with diethyl oxalate over HZSM-5. *Fuel Process. Technol.* **2009**, 90, 1220–1225.
- (42) Li, Y.; Xue, B.; He, X. Catalytic synthesis of ethylbenzene by alkylation of benzene with diethyl carbonate over HZSM-5. *Catal. Commun.* **2009**, 10, 702–707.
- (43) Gao, J.; Zhang, L.; Hu, J.; Li, W.; Wang, J. Effect of zinc salt on the synthesis of ZSM-5 for alkylation of benzene with ethanol. *Catal. Commun.* **2009**, 10, 1615–1619.
- (44) Kaeding, W. W. Shape-selective reactions with zeolite catalysts. V. Alkylation or disproportionation of ethylbenzene to produce *p*-diethylbenzene. *J. Catal.* **1985**, 95, 512–519.
- (45) Halgeri, A. B. Shape selective alkylation over pore engineered zeolite catalysts—IPCL's approach from concept to commercialization. *Bull. Catal. Soc. India* **2003**, 2, 184.
- (46) Guisnet, M.; Magnoux, P. *Zeolite Microporous Solids: Synthesis, Structure and Reactivity*; NATO ASI Series, Ser. C 352; Deraoune, E. G., Lemas, F., Naccache, C., Ramoa Ribeiro, F., Eds.; Kluwer Academic Publishing, Norwell, MA, 1992; p 457.
- (47) Lin, C. C.; Park, S. W.; Hatcher, W. J. *Ind. Eng. Chem. Process. Des. Dev.* **1983**, 22.
- (48) Siffert, S.; Gaillard, L.; Su, B. L. Alkylation of benzene by propene on a series of beta zeolites: Toward a better understanding of the mechanisms. *J. Mol. Catal.* **2000**, 10, 267–279.
- (49) Odedairo, T.; Al-Khattaf, S. Kinetic analysis of benzene ethylation over ZSM-5-based catalyst in a fluidized-bed reactor. Submitted for publication.
- (50) Du, Y.; Wang, H.; Chen, S. Study on alkylation of benzene with ethylene over  $\beta$ -zeolite catalyst to ethylbenzene by in situ IR. *J. Mol. Catal.* **2002**, 179, 253–261.
- (51) Bolton, A. P. Hydrocracking, isomerization, and other industrial processes. *Zeolite Chemistry and Catalysis*; ACS Monograph 171; Rabo, J. A., Ed.; American Chemical Society: Washington, DC, 1976; p 714.
- (52) Voorhies, A. Carbon formation in catalytic cracking. *Ind. Eng. Chem. Res.* **1945**, 37, 318–322.
- (53) Agarwal, A. K.; Brisk, M. L. Sequential experimental design for precise parameter estimation. 1. Use of reparameterization. *Ind. Eng. Chem. Process Des. Dev.* **1985**, 24, 203.
- (54) Levenspiel, O. *Chemical Reaction Engineering*, 3rd ed.; John Wiley & Sons: New York, 1999.
- (55) Atias, J. A.; Tonetto, G.; de Lasa, H. Catalytic conversion of 1,2,4-trimethylbenzene in a CREC riser simulator. A heterogeneous model with adsorption and reaction phenomena. *Ind. Eng. Chem. Res.* **2003**, 42, 4162–4173.

Received for review September 29, 2009

Revised manuscript received November 6, 2009

Accepted December 10, 2009